ELSEVIER
SAUNDERS

Thorac Surg Clin 14 (2004) 95–112

THORACIC
SURGERY
CLINICS

Radionuclide imaging of thoracic malignancies

Stanley J. Goldsmith, MD[a,b,*], Lale A. Kostakoglu, MD[a,b], Serge Somrov, MD[b], Christopher J. Palestro, MD[c,d]

[a]*Weill Medical College, Cornell University, 1300 York Avenue, New York, NY 10021, USA*
[b]*Division of Nuclear Medicine, New York Presbyterian Hospital, Weill Cornell Medical Center, 525 East 68th Street, New York, NY 10021, USA*
[c]*Albert Einstein College of Medicine, Yeshiva University, 1300 Morris Park Avenue, Bronx, NY 10461, USA*
[d]*Division of Nuclear Medicine, Long Island Jewish Medical Center, 270-05 76th Avenue, New Hyde Park, NY 11040, USA*

Thoracic masses are usually detected by chest radiograph or CT during a screening procedure, as part of a routine physical examination, or in the evaluation of some symptom or sign referable to the thoracic structures such as chest pain, cough, hemoptysis, wheezing, or dyspnea. The most common malignant tumor of the thorax is carcinoma of the lung, specifically the non–small-cell type, which includes adenocarcinoma and squamous cell carcinoma. Other masses requiring different management are also encountered, including small-cell lung carcinoma; bronchial carcinoid (benign and malignant); mediastinal masses, including thymoma, teratomas, lymphomas, and metastases from carcinomas such as breast, colon, head and neck tumors, thyroid carcinoma, and choriocarcinoma. In addition, carcinoma of the lung might be present as a second primary in patients known to have one of these other malignancies.

Traditionally, when a pulmonary mass has been identified a decision must be made regarding whether to perform a biopsy or surgical resection to characterize the lesion as a neoplasm versus granuloma or other inflammatory lesion and to determine a suitable course of management. In some instances surgical intervention is deferred and the lesion is reevaluated over time. Both approaches carry the risk of performing unnecessary surgery with the potential attendant morbidity or delaying evaluation with the associated risk of disease progression. This approach to management of the patient who has a thoracic lesion is rapidly changing with the development of nuclear medical imaging procedures that are capable of characterizing lesions according to their molecular biology. Radionuclide imaging is based on tissue or tumor function, metabolism, or other biochemical characteristics that provide information that is complementary to traditional diagnostic imaging techniques in terms of assessing if a lesion is malignant or not, and if malignant, determining the extent of disease.

In recent years radionuclide imaging has made great progress as a consequence of the development of novel radiolabeled compounds, which identify specific molecular processes and remarkable advances in the instrumentation used for acquisition and display. Nuclear medicine imaging has progressed to the point where it can provide crucial information about lesion biology and can thus play an integral part in the evaluation and management of the patient who has a suspected or known pulmonary malignancy, including noninvasive characterization of the solitary pulmonary nodule, assessment of the extent of disease in the patient who has a known malignancy, planning and optimizing radiation therapy, monitoring the response to treatment, and even predicting prognosis. State-of-the-art nuclear medicine imaging is clinically efficacious and cost-effective, leading to more accurate

* Corresponding author. Division of Nuclear Medicine, New York Presbyterian Hospital, Weill Cornell Medical Center, 525 East 68th Street, New York, NY 10021.
E-mail address: sjg2002@med.cornell.edu (S.J. Goldsmith).

1547-4127/04/$ – see front matter
doi:10.1016/S1547-4127(04)00034-9

diagnoses at less risk and lower cost to the patient and to society.

Technical advances

Nuclear medicine instrumentation

Nuclear medicine images, or scintigraphs, are generated by the external detection of emissions from radioactive isotopes that localize in certain tissues, organs, physiologic or pathophysiologic processes, or lesions. In the past, conventional nuclear medicine images were so-called planar images; data were recorded in multiple views: anterior, posterior, lateral, and oblique. Each image compressed the data obtained from the volume image into two dimensions, resulting in the loss of object contrast caused by the presence of background radioactivity (ie, radioactivity surrounding the object of interest). More recently, nuclear medicine has evolved toward tomographic imaging. In recent years clinicians and radiologists have become familiar with tomographic images as a result of the broad application of CT and, more recently, MRI (ie, transaxial slice images derived from reconstructed transmission data). Data are recorded in 360° geometry around the patient. Initially, backprojection techniques were used to create transverse, or transaxial, images (slices) that revealed the distribution of radioactivity, or, in the case of CT, absorption coefficient maps. Tomographic imaging is a more accurate representation of the actual distribution of radioactivity in a patient and results in improved image detail. Tomographic radionuclide imaging can be performed with single-photon or positron-emitting radionuclides.

Single-photon emission CT (SPECT) is the tomographic imaging technology employed with traditional radionuclides such as 99mTechnetium, ^{67}Gallium (^{67}Ga), and ^{201}Thallium (^{201}Tl). SPECT uses traditional collimated gamma camera positioning logic. Data are obtained at small angular intervals as the camera revolves around the patient. A gamma camera with a single detector must acquire data over 360°, whereas a device with two or three detector units requires that each head orbit only a fraction of the full circumference. Multihead systems permit greater data acquisition over a shorter period of time with a resultant improvement in image quality. Data acquired by the gamma camera are reconstructed into transaxial planes using sophisticated processing algorithms such as filtered backprojection and iterative reconstruction. In addition to the transaxial images, images from the coronal and sagittal planes are reconstructed readily. Modern computer capacity also makes it feasible to view three-dimensional, or volume, images.

Positron emission tomography (PET) is based upon the unique decay characteristics of positrons. A positron undergoes annihilation by combining with a negatively charged electron. As a result of this annihilation, two 511 keV gamma rays are emitted 180° apart. Special electronics determine if two recorded events are coincident, thus identifying the axis along which the two photons were emitted, which provides a significant advantage in terms of reconstructing the position of an event and allowing for the elimination of cumbersome lead collimators. In contrast to SPECT, in which single events are detected, PET makes use of two detector elements on opposite sides of the subject to detect coincident photons arising from the annihilation of a positron and electron. Most PET radiopharmaceuticals have short half-lives; consequently, until just a few years ago PET imaging was limited to centers that had cyclotron production facilities. After numerous investigational studies confirmed the value and cost-effectiveness of PET imaging with fluorine-18-fluorodeoxyglucose (^{18}FDG) in the management of patients who have tumors, third-party insurers and eventually governmental agencies approved the technique for reimbursement. Despite its short (2-hour) half-life, ^{18}FDG is now available from commercial sources in most of the United States.

Until recently, PET imaging devices cost more than $1 million and were available only at larger centers. The contribution of this technology to patient management, however, has been so significant that this situation is changing rapidly. The increased clinical demand for these studies has stimulated development of less costly instrumentation, and a spectrum of devices is now available including a $250,000 to $350,000 upgrade of conventional dual detector gamma camera systems, a 360° simultaneous acquisition imaging system that uses six large curvilinear sodium iodide crystals (costing approximately $1.3–1.5 million), and bismuth germanate multicrystal, multiring systems (costing $1.7–2.3 million).

Using a phantom in an experimental comparison of a gamma camera-based coincidence imaging system with a dedicated ring detector PET system, the dedicated PET system identified nodules as small as 6 mm in diameter, whereas the camera-based system resolved 1 cm and larger lesions [1]. There has been no direct comparison between imaging with the dedicated ring system and the less expensive devices in the clinical milieu. A meta-analysis published in 2001 found that the performance of the camera-based

system was comparable to that of dedicated PET in the evaluation of lung nodules in patients who had lesions greater than 1 cm in diameter [2]. Lesions as small as 7 mm in diameter can be detected on the dual detector coincident camera system, but overall image quality and lesion detection on a dedicated high-end system are significantly better. The ability to detect a lesion is based upon the resolution and sensitivity of the systems. In this regard the dedicated ring systems will regularly outperform (ie, show improved detection) dual detector systems even though coincident dual detector camera-based systems' imaging of ^{18}FDG are frequently useful to characterize lesions greater than 1 cm.

In summary, the dedicated ring detector systems represent the state-of-the-art in PET imaging with greater sensitivity for lesion detection. Nevertheless, dual detector camera-based systems provide access to ^{18}FDG imaging, and the positive predictive value is probably equivalent to that of the more expensive system. The negative predictive value of the dual detector system is likely to be somewhat less than that of the dedicated system because small lesions will not be detected as a result of volume averaging and reduced sensitivity.

As with most nuclear studies, PET images suffer from a paucity of anatomic detail. To maximize the accuracy of their interpretation, they should be read together with anatomic cross-sectional studies such as CT and MR, which has been accomplished by viewing the studies side-by-side on viewboxes or computer monitors or through the use of fusion software that allows direct superimposition of the images. Recently, instruments have been engineered that acquire PET and CT images. Patients undergo sequential PET and CT studies on the same instrument during the same imaging session. Fused PET and CT images and PET and CT images alone can be viewed on a slice-by-slice basis. Though costly and still new, these devices have already demonstrated that they have advantages in terms of accuracy and confidence in interpretation, and they are likely to eventually replace PET-only and CT-only devices [3].

Radionuclides

In the past, nuclear medicine assessed thoracic masses with ^{67}Ga citrate and, more recently, with ^{201}Tl and ^{99m}Technetium (^{99m}Tc)-MIBI [4,5]. ^{67}Ga scintigraphy is positive in inflammatory and neoplastic lesions. Despite this degree of nonspecificity, the technique was useful but limited in application because of the comparatively poor resolution achieved with this radionuclide. Tumor localization of ^{201}Tl and ^{99m}Tc-MIBI is a consequence of perfusion and rapid extraction of these tracers from tumor tissue. ^{99m}Tc-MIBI has the advantage of greater photon flux than ^{201}Tl because a larger dose can be given because of the shorter (6-hour) half-life. The 140 keV photon energy is more suitable for imaging than the lower energy photons of ^{201}Tl. Furthermore, ^{99m}Tc-MIBI binds to intracellular elements, providing improved target to background ratios.

These techniques, however, provide limited improvement over CT or MRI in terms of detection of disease. ^{99m}Tc-MIBI could also be used to characterize tumor multiple-drug resistance by examining the retention or washout of ^{99m}Tc-MIBI over time because ^{99m}Tc-MIBI is eliminated from tissue by the same p51 glycoprotein multiple drug resistance (MDR) mechanism [6].

Any historical review should include Iodine-131 (^{131}I), which is used to detect metastases from thyroid carcinoma—even in patients who have a negative chest radiograph or CT examination (Fig. 1). Thyroid carcinoma frequently has a subtle micronodular appearance, although it might occasionally appear as single or multiple nodules. It is important to correctly identify lung metastases from thyroid carcinoma because they respond to radionuclide therapy with ^{131}I.

Radiolabeled peptides

Radiolabeled compounds that bind to receptors present in normal and abnormal tissues form the basis of receptor imaging. Tumor expressing receptors can be visualized with radiolabeled antibodies or radiolabeled messenger molecules. To date, the most successful of these agents has been radiolabeled analogs of regulatory peptides. Regulatory peptides are small, easily diffuseable, naturally occurring substances that possess a wide spectrum of receptor-mediated actions. High-affinity receptors for these peptides are present on many neoplasms. These receptors offer molecular targets for diagnosis and therapy [7]. Currently, two radiolabeled peptides, Octreoscan (Mallinkrodt, St. Louis, Missouri) and Neotect (Diatide, Londonderry, New Hampshire), both of which are somatostatin analogs, are approved for diagnostic use in the United States.

Somatostatin is an endogenous neuropeptide that exists in two forms: a 14 amino acid form and a 28 amino acid form. It is synthesized in the central nervous system, the hypothalamopituitary axis, the gastrointestinal tract, the pancreas, and the immune system. Somatostatin receptors, of which there are five subtypes, are present on many cells, particularly

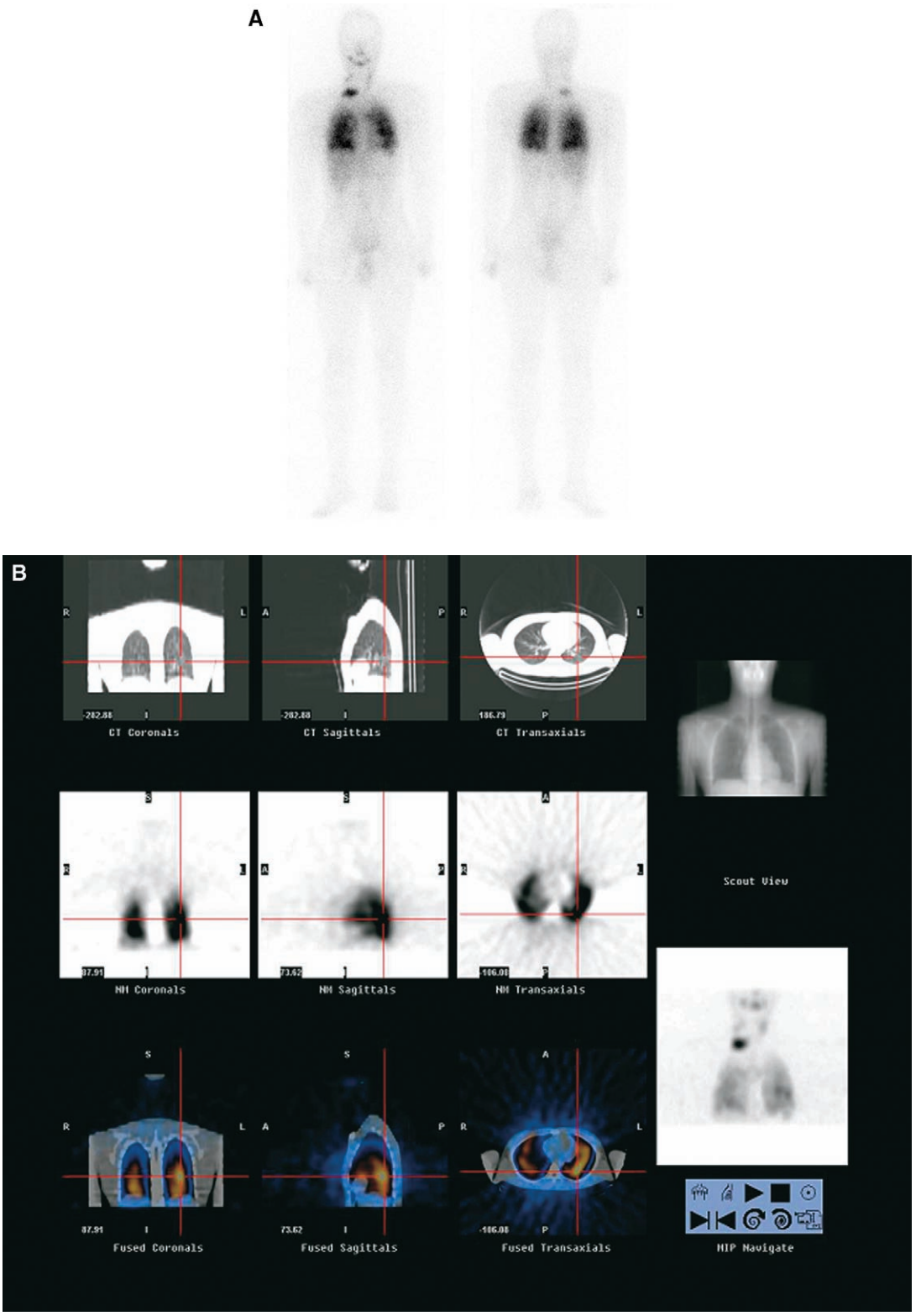
A
B
CT Coronals
CT Sagittals
CT Transaxials
Scout View
NM Coronals
NM Sagittals
NM Transaxials
Fused Coronals
Fused Sagittals
Fused Transaxials
MIP Navigate

those of neuroendocrine origin. These receptors have also been identified on activated lymphocytes and the vasa recta of the kidney. All five receptor subtypes bind to naturally occurring somatostatin with nearly identical affinity [8,9].

In addition to their presence on normal tissues, somatostatin receptors are expressed on a wide variety of human tumors. Three main groups of tumors have been identified as having the highest density of somatostatin receptors. Neuroendocrine tumors, including islet cell tumors, gastrinomas, pheochromocytomas, paragangliomas, and carcinoid tumors are one group. Central nervous system tumors such as astrocytomas and meningiomas represent another group. The third group of tumors that possess somatostatin receptors consists of lung carcinoma (small-cell and non–small-cell), breast tumors, lymphomas, and renal cell carcinoma.

The short biologic half-life of somatostatin (~ 1 min) precludes its use for diagnostic or therapeutic purposes, which led to the development of synthetic somatostatin analogs that had longer biologic half-lives. Octreotide is an eight amino acid analog with a high affinity for somatostatin subtype receptors 2 and 5 but a decreased affinity for subtype 3 and no affinity for subtypes 1 and 4 [7]. Octreoscan is produced by radiolabeling diethylene tetra amine penta acetic acid (DTPA)-pentetreotide (a derivative of octreotide) with Indium-111 (^{111}In) and is used to image somatostatin receptor-bearing tumors. Extensive studies in large numbers of patients have shown that somatostatin receptor scintigraphy (SRS) with ^{111}In DTPA-pentetreotide is most useful in detecting and staging neuroendocrine tumors [8–10].

In the thorax, SRS is especially useful in small-cell lung carcinoma and bronchial carcinoid. In small-cell lung carcinoma, the sensitivity of SRS is more than 90% for the primary lesion. More than half of metastatic lesions, however, lose their somatostatin receptor expression as a consequence of dedifferentiation and increasing malignancy [11]. Visualization of metastatic small-cell lung carcinoma lesions indicates that the tumor is relatively well differentiated, whereas nonvisualization is associated with dedifferentiation and a poorer prognosis. Thus, it is possible, using scintigraphic imaging, to not only localize lesions but also to determine prognosis through in vivo tissue characterization.

Bronchial carcinoid is an uncommon neoplasm, accounting for less than 5% of all lung tumors. Thought at one time to be benign, this entity is, in fact, a low-grade, slow-growing, malignant neoplasm that has the potential for local invasion and distant metastatic spread (Fig. 2). Several investigators have reported on the role of SRS in bronchial carcinoid [12–14]. In a series of 21 patients, SRS revealed all eight primary lesions at the time of diagnosis, demonstrated disease in all five patients who had recurrent or metastatic disease (including two patients who were asymptomatic at the time of imaging), and identified an increase in tumor size in two patients who had unresectable disease [13]. In a series of 31 patients who had bronchial carcinoid, six patients (nearly 20%) had lesions that were identified only on SRS. Lesions identified only with SRS included pulmonary, hepatic, and osseous. In two patients who had inconclusive CT studies, SRS correctly excluded recurrent disease. Only two pulmonary lesions, both in the same patient, which were detected with other modalities were not detected with SRS [12].

The implications of the findings in these investigations are important. Although sensitive for the detection of neuroendocrine tumors, SRS cannot be used for diagnosis because other lung tumors also express somatostatin receptors. SRS is used to guide patient management. For example, the exquisite sensitivity of SRS can determine whether or not, at the time of diagnosis, curative surgery is possible. In patients who have recurrent disease, localized surgical resection has met with some success. The ability to identify recurrent disease in asymptomatic patients suggests that SRS might be useful for identifying individuals who have recurrent disease when they are still amenable to surgery. This is of value to determining if metastatic disease is limited to

Fig. 1. Twenty-year-old man post-thyroidectomy for differentiated thyroid carcinoma was found to have a palpable mass in the right supraclavicular region. The mass was positive on diagnostic ^{131}I imaging. Following dosimetry to determine the bone marrow radiation absorbed dose, the patient received 300 mCi of ^{131}I. (*A*) Whole-body scan 1 week post ^{131}I therapy confirming ^{131}I uptake in the right supraclavicular mass and demonstrating unexpected diffuse uptake throughout both lung fields. Uptake had not been recognized on diagnostic imaging with a lower dose of ^{131}I. (*B*) SPECT images of the same patient's thorax using a dual detector system with a low-output CT device (GE Millenium Hawkeye, General Electric Medical Systems, Milwaukee, Wisconsin, USA). *Top row:* CT images in the coronal, sagittal, and transaxial plane. *Middle row:* ^{131}I tomographic images corresponding to CT slices. *Bottom row:* Fused CT plus ^{131}I images. On the upper right, the scout radiograph of the chest is negative; on the lower right is the anterior rendering of the ^{131}I volume (all images summed) display. (Courtesy of Division of Nuclear Medicine, Department of Radiology, New York Presbyterian Hospital, Weill Cornell Medical Center, New York, NY).

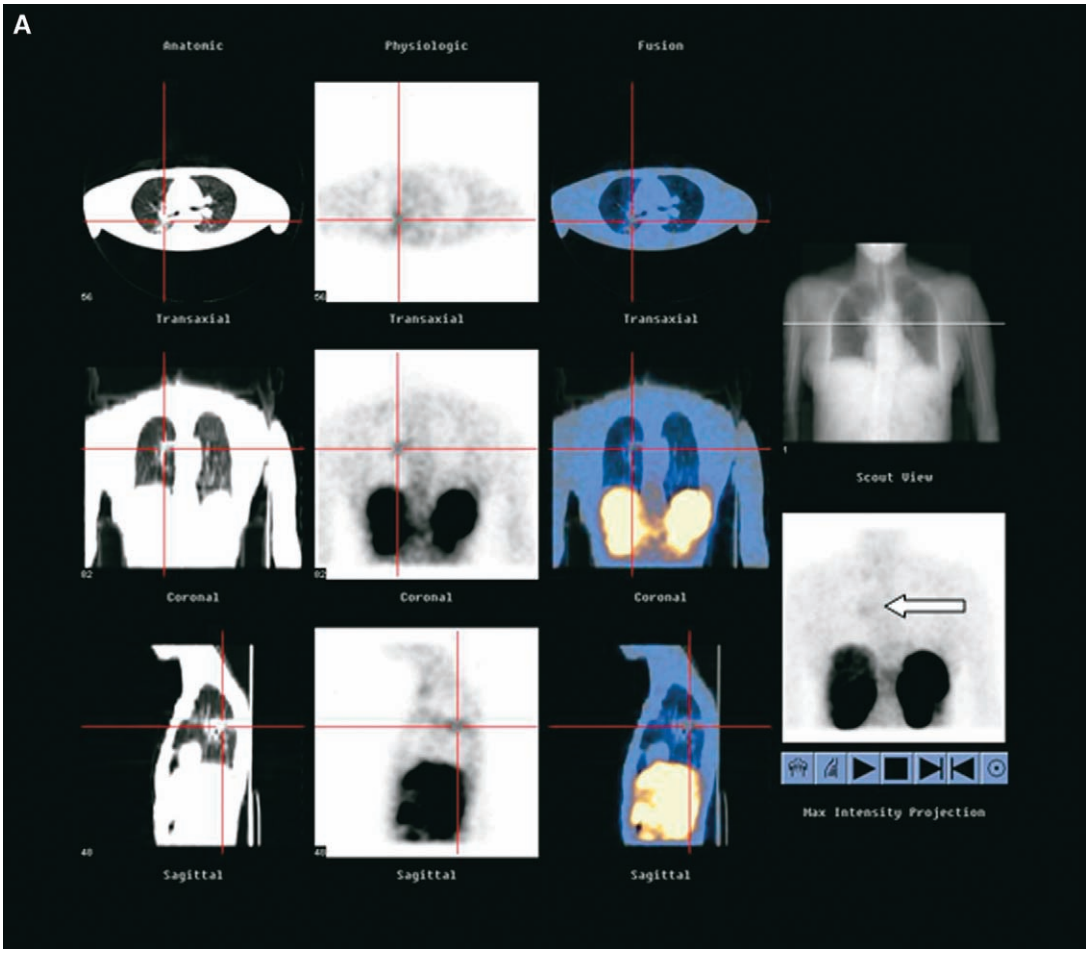
A
Anatomic
Physiologic
Fusion
Transaxial
Transaxial
Transaxial
Scout View
Coronal
Coronal
Coronal
Sagittal
Sagittal
Sagittal
Max Intensity Projection


B

the liver, because in some cases current surgical practice makes it possible to consider liver transplantation. Extrahepatic metastatic disease is a contraindication, however, and SRS is useful for identifying or excluding patients for this procedure. Finally, determining the presence or absence of somatostatin receptors with SRS identifies patients who are likely to respond to medical therapy.

Another radiolabeled somatostatin analog, ^{99m}Tc-depreotide (Neotect), has been developed. ^{99m}Tc-depreotide is a synthetic cyclic six amino acid peptide labeled with technetium-99m and is approved for the differential diagnosis of the solitary pulmonary nodule. This agent is a high-affinity ligand for human somatostatin receptor subtype 3, with in vitro characteristics that suggest it should also be useful for imaging the extent of disease in patients who have non–small-cell and small-cell lung carcinoma. In a series of 30 patients who had solitary pulmonary nodules at least 1 cm in diameter who were at high risk for lung carcinoma but had indeterminate CT criteria, the sensitivity of ^{99m}Tc-depreotide for detecting malignancy was 93% (12/13), the specificity was 88% (15/17), and the accuracy was 90% (27/30). The study was falsely negative in one patient who had squamous cell carcinoma and falsely positive in two patients who had necrotizing granulomas [15]. In a 114-patient multicenter trial, the sensitivity, specificity, and accuracy of ^{99m}Tc-depreotide was 97% (85/88), 73% (19/26), and 91% (104/114), respectively. The three false-negative lesions were adenocarcinomas; two were primary lung lesions and one was thought to be metastatic colon carcinoma. Six false-positive results were granulomatas; the seventh was a hamartoma. The data suggest that ^{99m}Tc-depreotide scintigraphy is a sensitive and accurate method for the noninvasive evaluation of the solitary lung nodule that is at least 1 cm in diameter [16].

An analysis of the cost-effectiveness of ^{99m}Tc-depreotide imaging in 114 patients who had indeterminate lung nodules found that in individuals who had a 50% probability of having a malignancy, CT alone and CT followed by ^{99m}Tc-depreotide scintigraphy showed an incremental cost-effectiveness ratio of approximately $11,200 and $8600, respectively, per year of life saved. Radiograph follow-up is only cost-effective when the probability of malignancy is less than 0.14, whereas CT alone is cost-effective when the probability of malignancy is 0.71 to 0.90. When the probability of malignancy is greater than 0.90, thoracotomy is the best choice. CT plus ^{99m}Tc-depreotide is the most cost-effective strategy, resulting in a savings of $68 to $1800 for the majority of patients, depending on the risk, when the probability of malignancy is between 0.14 and 0.71. Based on a Medicare reimbursement of approximately $900, ^{99m}Tc-depreotide imaging of pulmonary nodules that are indeterminate by CT criteria would result in an annual savings of up to $54 million compared with selecting patients for thoracotomy based on CT results alone [17]. Another beneficial aspect of this approach would be a decrease in the cost and complications of unnecessary needle biopsies.

Currently, no data are available on the accuracy of ^{99m}Tc-depreotide imaging for evaluating lesions smaller than 1 cm in diameter, nor on its role in the staging of lung carcinoma, monitoring response to therapy, or detecting recurrent disease.

Fluorodeoxyglucose

Fluorodeoxyglucose (FDG) is a structural analog of 2-deoxyglucose, which, like glucose, is transported into cells and phosphorylated by a hexokinase to FDG-6 phosphate. FDG accumulates intracellularly in proportion to the glycolytic rate of the cell. FDG uptake by tumor cells is also related to the presence of increased glucose transporter molecule expression at the tumor cell surface and to increased levels of hexokinase in these cells. Labeled with the positron emitter fluorine-18 (^{18}F), FDG is useful for detecting areas of normal and abnormal glucose metabolism. Although it is filtered by the glomerulus, FDG is not reabsorbed in the proxi-

Fig. 2. (*A*) ^{111}In-DTPA-pentetreotide (Octreoscan) SPECT scintigraphy in a 67-year-old woman who had a history of pulmonary carcinoid; status right upper lobe (RUL) resection 30 months earlier with negative follow-up scans. *Left column:* CT acquired on GE Millennium dual detector camera system with Hawkeye configuration (transaxial, coronal, and sagittal slices). *Middle column:* Corresponding ^{111}In images. *Right column:* Fused images. *Extreme right*: Scout radiograph and ^{111}In volume display. Note ^{111}In-DTPA-pentetreotide-positive mass in region of right hilum superimposed on superior portion of CT density. (Courtesy of Division of Nuclear Medicine, Department of Radiology, New York Presbyterian Hospital, Weill Cornell Medical Center, New York, NY). (*B*) ^{111}In-DTPA-pentetreotide (Octreoscan) planar scintigraphy of the thorax and abdomen in a 44-year-old man who had small-cell lung carcinoma. Tumor foci are identified in the right hilar area, the left paratracheal area, and the left anterior cervical triangle. (Courtesy of Division of Nuclear Medicine, Department of Radiology, Long Island Jewish–Hillside Medical Center, New Hyde Park, NY).

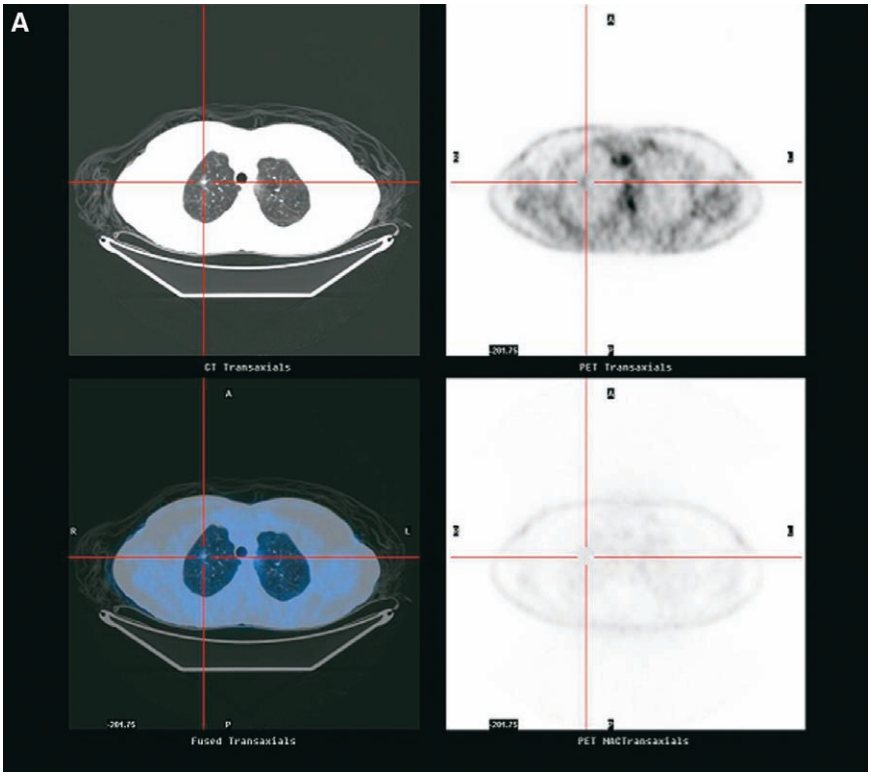
A
CT Transaxials
PET Transaxials
Fused Transaxials
PET NACTransaxials

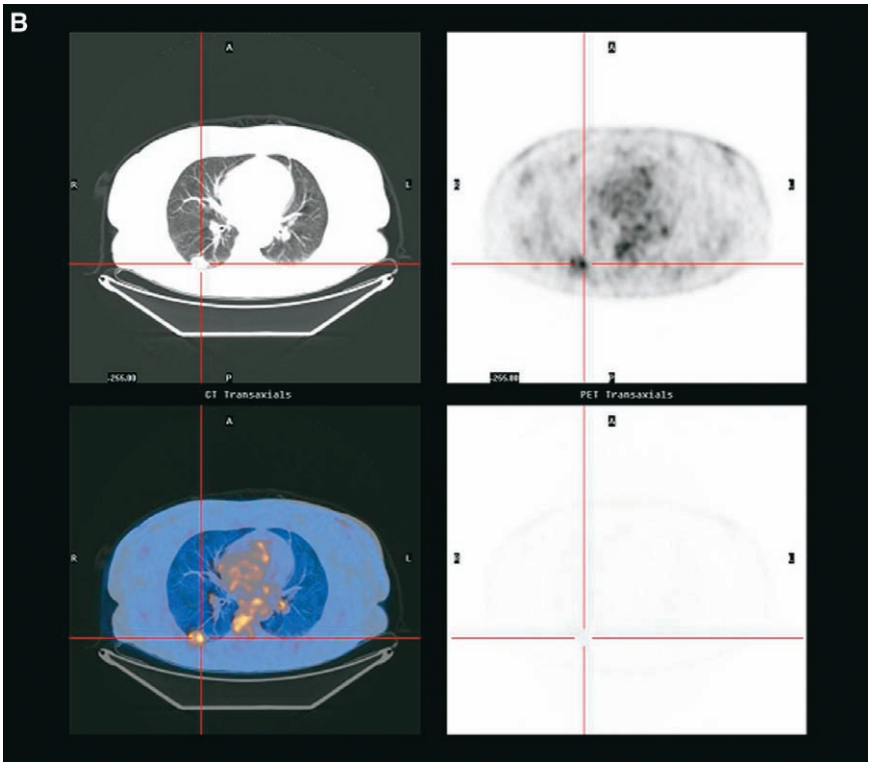
B
CT Transaxials
PET Transaxials

mal renal tubules, and the blood concentration of this compound falls quickly, providing high contrast between foci of increased glucose metabolism and background activity within 1 hour of injection. Many tumors are characterized by increased anaerobic glucose metabolism, and ^{18}FDG provides a sensitive tool for their detection. In lung cancer, ^{18}FDG-PET imaging provides important information about the diagnosis, pretreatment staging, and assessment of the effects of treatment in this entity. Its potential role in predicting prognosis is currently being assessed.

Fluorine-18-fluorodeoxyglucose–positron emission tomography and lung carcinoma

Nearly 1 million new cases of lung cancer are diagnosed annually, principally in developed nations. At the time of diagnosis, the disease has already spread to adjacent hilar or mediastinal lymph nodes in about 25% of patients, and 35% to 45% of patients have distant metastases [18,19]. A systematic approach to the diagnosis, staging, and treatment of lung cancer optimizes therapy for each individual patient.

Diagnosis

The diagnosis of lung carcinoma, as for any other tumor, is the first challenge with which the clinician is faced when presented with a patient suspected of having this entity. While morphologic imaging studies such as planar radiographs, CT, and MRI can detect a pulmonary lesion, they often cannot determine whether it is benign or malignant. Only about one third of pulmonary nodules can be diagnosed as benign or malignant on the basis of CT criteria alone. In the other two thirds, diagnosis depends on more invasive procedures such as bronchoscopy and percutaneous CT-guided transthoracic needle aspiration [20,21]. The overall sensitivity of bronchoscopy in detecting malignancy is about 65%. If transbronchial biopsy is performed, the sensitivity approaches 80% [22,23]. The sensitivity of the CT-guided procedure is greater than 90% if an adequate sample is obtained. The frequency of sampling errors depends on the size and location of the lesion and on operator expertise. The most common complication of needle biopsy is pneumothorax, which occurs in up to10% of patients [24].

The characterization of a pulmonary nodule as benign or malignant with ^{18}F-FDG-PET was one of the earliest oncologic applications investigated, and its value for this purpose is now well established (Fig. 3). The sensitivity and specificity of ^{18}FDG-PET imaging in the evaluation of solitary lung nodules ranges from 82% to 100% and 63% to 90%, respectively [25–34]. A meta-analysis of 1474 pulmonary lesions found that the mean sensitivity and specificity of ^{18}FDG-PET was 96% and 74%, respectively [2].

Several factors affect the sensitivity of ^{18}FDG-PET imaging for the diagnosis of malignancy. Lesion visualization depends on the amount of ^{18}FDG incorporated into the tumor. Abnormalities typically present as areas of focally increased activity, colloquially referred to as hotspots. Images can be analyzed visually and semiquantitatively. In the chest, mediastinal blood pool activity is often used as the reference point. Uptake in a lesion that is more intense than mediastinal blood pool activity is likely to be malignant, whereas activity equal to or less than mediastinal blood activity is likely to be benign. It is also possible to quantify activity by calculating the standardized uptake value (SUV), which reflects the ratio of activity per estimated tumor volume to the total activity administered to the patient, corrected for the lean body mass. Although not absolutely diagnostic, SUVs greater than 2.5 are often associated with malignancy, and malignant lesions generally have SUVs greater than 2.5. Fractional ^{18}FDG uptake is affected by specific tumor metabolic activity. Consequently, tumors such as bronchioalveolar cell carcinoma and bronchial carcinoid with relatively low metabolic activity might not concentrate sufficient ^{18}FDG to be identified as malignant. Nevertheless, subsets of these tumor types (bronchioalveolar carcinoma and carcinoid or other neuroendocrine tumors) might be metabolically active and identifiable as malignant on ^{18}FDG imaging. Meta-

Fig. 3. (*A*) Fifty-three-year-old woman who had a recently diagnosed RUL pulmonary nodule. Patient had a 30 pack-year history of cigarette smoking. The ^{18}FDG-PET images are entirely normal. The patient will continue to be followed. (*B*) Sixty-five-year-old man who had a history of an right lower lobe (RLL) solitary pulmonary nodule that had been followed since 2000. The nodule had increased in size recently. ^{18}FDG-PET images demonstrate a hypermetabolic focus consistent with a malignant process. There is no evidence of regional lymph node involvement, indicating that the patient is an appropriate surgical candidate. (Courtesy of Division of Nuclear Medicine, Department of Radiology, New York Presbyterian Hospital, Weill Cornell Medical Center, New York, NY).

static differentiated thyroid carcinoma can be positive or negative on ^{18}FDG imaging depending, apparently, on the degree of biologic aggressiveness at the time of imaging. The degree of tumor aggressiveness is reflected in the metabolic rate. Although some well-differentiated adenocarcinomas might demonstrate only modest accumulation of ^{18}FDG, their SUVs are nevertheless typically in the malignant range [35]. Sensitivity is also affected by lesion size. Lesions below the limits of resolution of PET scanners (currently about 4–8 mm depending upon the system hardware configuration) might not be detected [36,37]. The lesion intensity and the measured SUV will be blunted by the phenomenon known as volume averaging, in which the absolute uptake in a lesion below the spatial resolution of the system is distributed over the minimal resolution area, resulting in an apparent lowering of the activity per pixel. Sensitivity is also adversely affected by hyperglycemia. Presumably, competitive inhibition results from elevated serum glucose levels, reducing ^{18}FDG uptake. In addition to this direct competitive effect, the insulin response to the glucose level is greatest in acute hyperglycemia. This response promotes muscle and hepatic uptake of glucose and ^{18}FDG. Chronic hyperglycemia has a lesser effect on FDG uptake by tumors [38]. In patients who are diabetic, control of the disease should be optimized and serum glucose levels checked before injecting ^{18}FDG. In general, patients who have serum glucose levels above 250 mg/dL should probably not undergo ^{18}FDG imaging until serum glucose levels have been controlled.

Increased glycolysis is not unique to tumors, however; it occurs in benign conditions such as granulomas, histoplasmosis, coccidioidomycosis, and pneumonia, in which false-positive findings are observed [39–42]. Some data suggest that the specificity of the overall results can be improved by performing dual time point imaging. ^{18}FDG uptake in tumor tends to increase over time, whereas inflammation tends to remain constant or decrease over time [43]. By acquiring a second set of images about 1 hour after the first set, it might be possible to distinguish ^{18}FDG uptake in benign inflammatory conditions from that in tumors.

^{18}FDG-PET obviates the need for invasive biopsy in many patients who have lung nodules. To be used for this purpose, the test must have a high negative predictive value, which depends not only on sensitivity and specificity but also on the pretest likelihood of malignancy. Using decision analysis modeling, it has been shown that only patients who have a 50% or lower pretest likelihood of cancer should undergo ^{18}FDG-PET imaging. If the pretest likelihood of malignancy is more than 50%, the posttest probability of disease will exceed 10% even if the ^{18}FDG images are negative for one reason or another (ie, size, metabolic activity, blood glucose), and histopathologic evaluation will be necessary regardless of the ^{18}FDG-PET results [44]. Because there is always the risk of a false-negative result even when the negative predictive value is high (eg, a negative ^{18}FDG-PET study in a patient who has <50% pretest probability), patients who have lung nodules and negative ^{18}FDG-PET studies should undergo routine clinical and imaging follow-up every 6 to 12 months (as with other potentially malignant lesions) to monitor for any increase in the lesion size.

Staging

Pretreatment staging of non-small cell lung carcinoma (NSCLC) is necessary to assess prognosis and to determine appropriate therapy (Figs. 4–6). For example, patients who do not have mediastinal lymph node or distant metastatic disease usually undergo surgical resection of the tumor, whereas patients who have mediastinal or distant disease can undergo induction chemotherapy or radiotherapy before surgery. CT imaging is used to anatomically define the extent of the primary tumor and pleural or chest wall involvement and is superior to FDG-PET for these purposes because of its inherently better spatial resolution and delineation of normal structures and anatomic detail. CT identification of hilar and mediastinal lymph node involvement is less than optimal, however, because it depends upon lesion size. Using a size criterion of 1 cm as the threshold for identification of malignant disease leads to under- and overstaging. Normal-sized lymph nodes that are infiltrated by tumor will not be recognized, whereas lymph nodes that are enlarged secondary to benign processes will be incorrectly interpreted as containing tumor. The sensitivity, specificity, and accuracy of mediastinal staging by CT, as reported in a meta-analysis, is approximately 60%, 77%, and 65%, respectively [45]. In a prospective study, the sensitivity and specificity of CT was 52% and 69%, respectively [46]. Mediastinoscopy has, consequently, been the reference technique for mediastinal lymph node staging.

The accuracy of ^{18}FDG-PET for assessment of mediastinal nodal involvement has been investigated extensively. The sensitivity and specificity of the procedure, when reported as positive or negative for the ipsilateral or contralateral side, have ranged form 67% to 92% and 86% to 97%, respectively [47–52]. When analyzed by nodal stations, the reported results

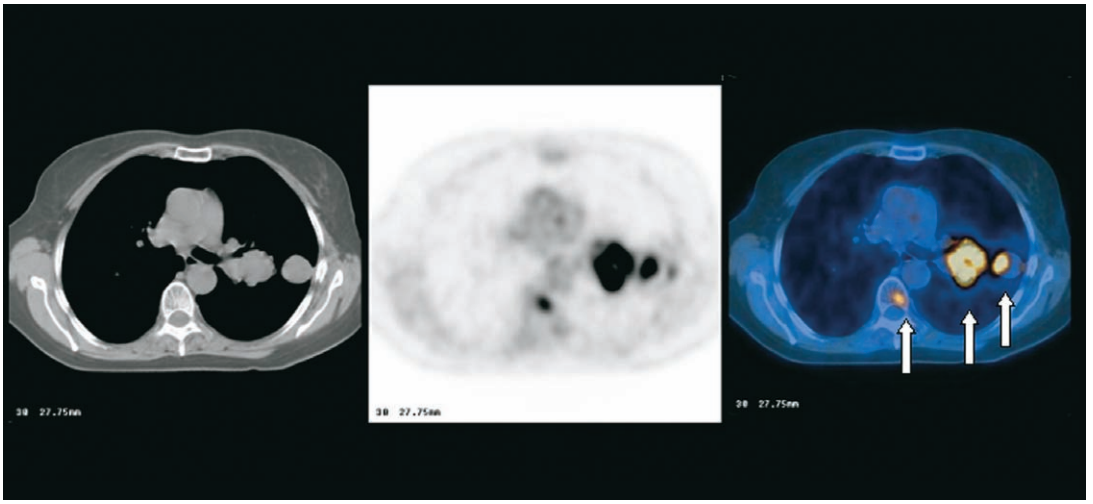

Fig. 4. Selected transaxial slice demonstrating ^{18}FDG-PET images in a 68-year-old woman who smoked 1 pack of cigarettes per day for many years. She presented to her primary care physician with complaints of back pain but was otherwise in good health. A chest radiograph revealed a hilar mass and lung nodules. Transbronchial biopsy was positive for poorly differentiated non–small-cell lung carcinoma. The patient was referred for evaluation of the extent of disease. The so-called hilar mass was actually the primary lung tumor adjacent to hilar structures with a nearby second and third focus. A metastatic lesion in the vertebral body was also demonstrated. The accompanying CT image shows multiple tumor masses and evidence of a sclerotic lesion in the vertebral body (lung CT window). ^{18}FDG-PET indicates the extent of viable tumor. Recently, radiation treatment plans using intensity modulated radiation therapy (IMRT) were designed to provide booster radiation doses to the well-circumscribed viable tumor defined by ^{18}FDG-PET as opposed to simply delivering the prescribed dose to the entire CT defined tumor volume. (Courtesy of Jacqueline Brunetti, MD, Department of Radiology, Holy Name Hospital, Teaneck, NJ).

are similar. A study published in 1999 compared ^{18}FDG-PET and CT in 75 patients prospectively [53]. ^{18}FDG-PET imaging and CT were concordant in 39 patients, correctly in 35 of the 39 patients but overstaging in two patients and understaging in two patients. The results of the two studies were discordant in 36 patients; ^{18}FDG-PET was correct in 28 of these patients. Hence, ^{18}FDG-PET was correct in 63 of 75 patients, whereas CT was correct in only 43 of 75 patients. In a meta-analysis of staging, the mean sensitivity and specificity of ^{18}FDG-PET was 79% (±3%) and 91% (±2%) respectively, versus 60% (±2%) and 77% (±2%), respectively, for CT [45].

The anatomic–functional correlation of ^{18}FDG-PET and CT images using fusion imaging (in which the two studies are obtained sequentially on the same instrument) will undoubtedly further refine the classification of patients who have nodal or mediastinal disease by separating the primary tumor from adjacent lymph nodes, differentiating hilar from adjacent mediastinal nodes, and precisely identifying the mediastinal lymph node groups involved. It is especially important to differentiate between N1 and N2 disease because the former is directly operable and the latter is not. These conclusions are based upon traditional methods of staging. The identification of N1 disease by ^{18}FDG-PET at an earlier time than would have been possible with CT provides a basis for modifying surgical resection to include these positive nodes rather than to conclude that there is no nodal involvement based upon CT imaging alone.

Patients who have distant, or systemic, metastases at the time of diagnosis cannot be cured by surgery and are not likely to achieve a long-term remission. Despite the fact that the incidence of distant recurrence after complete removal of the primary tumor is at least 20%, conventional staging procedures performed at the time of diagnosis are generally unrewarding [54]. Because the diagnostic yield of anatomic imaging is low, ^{18}FDG-PET offers a rapid method for whole-body imaging that identifies systemic metastatic disease effectively. ^{18}FDG-PET detects distant disease in up to 15% of patients who have negative conventional staging procedures [52,55,56]. In addition to improving the detection of disease, a negative study can also exclude disease in patients who have false-positive or equivocal conventional imaging results.

Adrenal masses are identified on CT in up to 20% of patients who have NSCLC, and ^{18}FDG-PET can

accurately characterize the lesion as benign or malignant (Fig. 5). In one series of 27 patients, ^{18}FDG-PET was 100% sensitive and 80% specific for adrenal metastases [57]. The high negative predictive value of this technique can reduce the need for routine biopsy of adrenal masses.

Lung carcinoma frequently metastasizes to bone (Fig. 5). Radionuclide bone scintigraphy using ^{99m}Tc-methylene diphosphonate (^{99m}Tc-MDP) had been considered to be the procedure of choice for the clinical assessment of possible skeletal involvement. Bone metastases from NSCLC are often osteolytic,

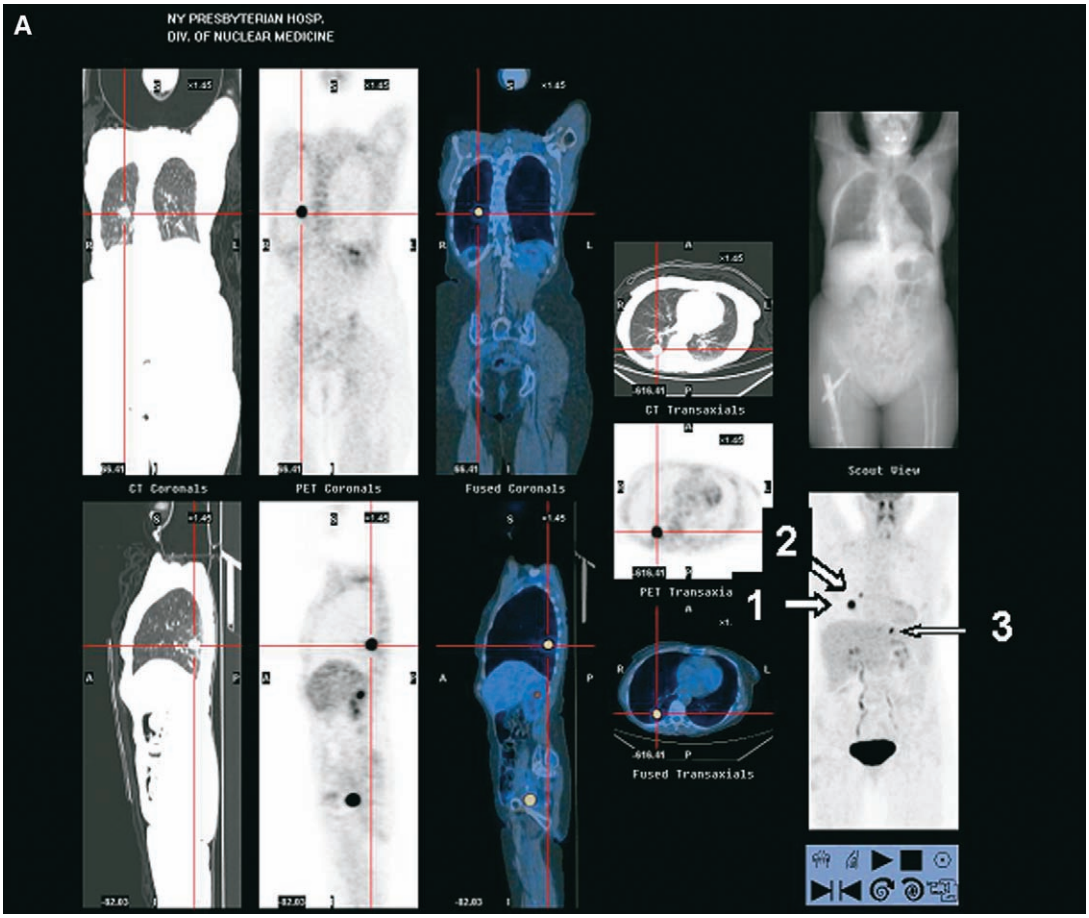

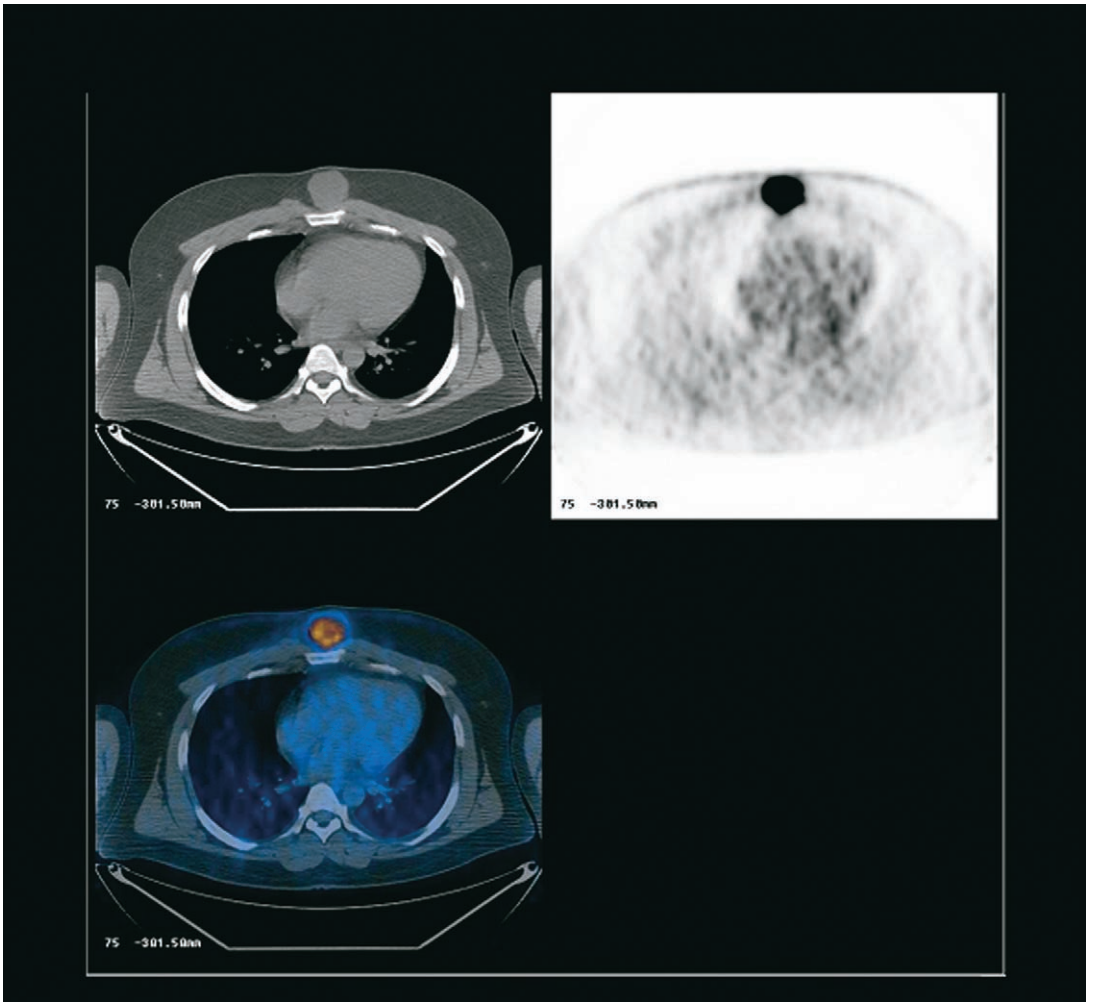

Fig. 6. ^{18}FDG-PET, CT, and fusion transaxial images in a patient presenting with a chest wall mass. No satellite lesions or lymph node involvement was demonstrated; biopsy demonstrated chondrosarcoma. (Courtesy of Division of Nuclear Medicine, Department of Radiology, New York Presbyterian Hospital, Weill Cornell Medical Center, New York, NY).

and ^{18}FDG is reportedly more sensitive than conventional radionuclide bone imaging for this type of bone lesion. In addition, ^{18}FDG-PET produces fewer false-positive results in degenerative, inflammatory, and posttraumatic bone disease [58,59]. False-positive ^{18}FDG-PET results have been reported with acute fractures [60].

Liver metastases are readily detected by conventional imaging studies. ^{18}FDG-PET is most useful for resolving abnormalities that are indeterminate on

Fig. 5. (*A*) ^{18}FDG-PET images from a 62-year-old woman admitted with confusion who was a cigarette smoker, 1 pack/day for 50 years. A solitary pulmonary nodule on the chest radiograph was subsequently confirmed as adenocarcinoma on biopsy. Brain metastases were present on MRI. A CT of the chest and abdomen to the kidneys was interpreted as normal except for the primary pulmonary lesion. Coronal, sagittal, and transaxial ^{18}FDG-PET images are triangulated (*crosshairs*) on the primary lesion (*arrow 1*). A metastatic ipsilateral hilar lymph node is identified (*arrow 2*), and a metastasis to the left adrenal is also seen (*arrow 3*), although the right hilar node and left adrenal are normal on CT. (*B*) Transaxial slices (CT, PET, and fusion images) demonstrating adrenal metastasis in a normal left adrenal gland on CT examination. (Courtesy of Division of Nuclear Medicine, Department of Radiology, New York Presbyterian Hospital, Weill Cornell Medical Center, New York, NY).

conventional studies [61]. Although ^{18}FDG-PET can detect lung metastases, CT has higher resolution and is less affected by respiratory motion than ^{18}FDG-PET images. For optimal detection of brain metastases, a dedicated brain acquisition should be performed. This additional study is probably not routinely warranted in light of the low incidence of brain metastases in asymptomatic patients and because of the excellent results obtained with contrast-enhanced CT and MRI.

The effectiveness of ^{18}FDG-PET in the staging of NSCLC is a direct result of its ability to detect metastases that are not apparent on conventional imaging modalities and to clarify the etiology of indeterminate lesions found on CT. It has been estimated that ^{18}FDG-PET imaging results in changes in patient management in 20% to 40% of patients. Perhaps most important is the exclusion of surgery in up to 15% of patients as a result of the detection of distant metastases [56,62–64].

Treatment and prognosis

In addition to assisting in the identification of individuals who are suitable for curative surgery, ^{18}FDG-PET is also used for radiotherapy planning by defining functional tumor volume and providing an outline of the radiotherapy volume for inclusion of tumor and sparing of adjacent, uninvolved structures. In one series, changes in staging were made in 33% of patients and changes in radiation treatment vol-

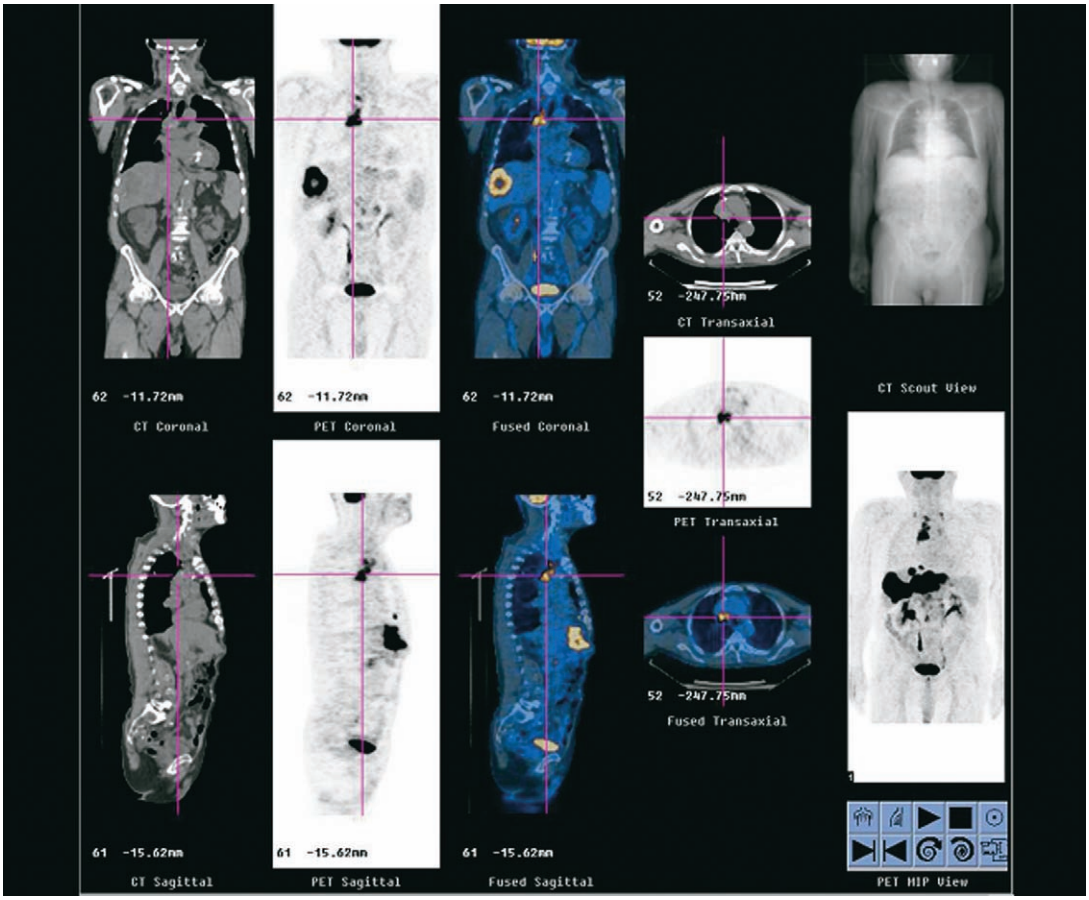

Fig. 7. ^{18}FDG-PET, CT, and fusion images from a 73-year-old man who had a history of colon carcinoma that was resected 4 years earlier followed by a course of chemotherapy. The patient now has an elevated serum carcino embryonic antigen (CEA) value and suspicion of a mediastinal mass. A hypermetabolic (increased ^{18}FDG) mass is seen in the right anterior mediastinum and a large mass is seen in the liver. These findings are metastatic colon carcinoma. The chest mass is indistinguishable from a second primary neoplasm. (Courtesy of Division of Nuclear Medicine, Department of Radiology, New York Presbyterian Hospital, Weill Cornell Medical Center, New York, NY).

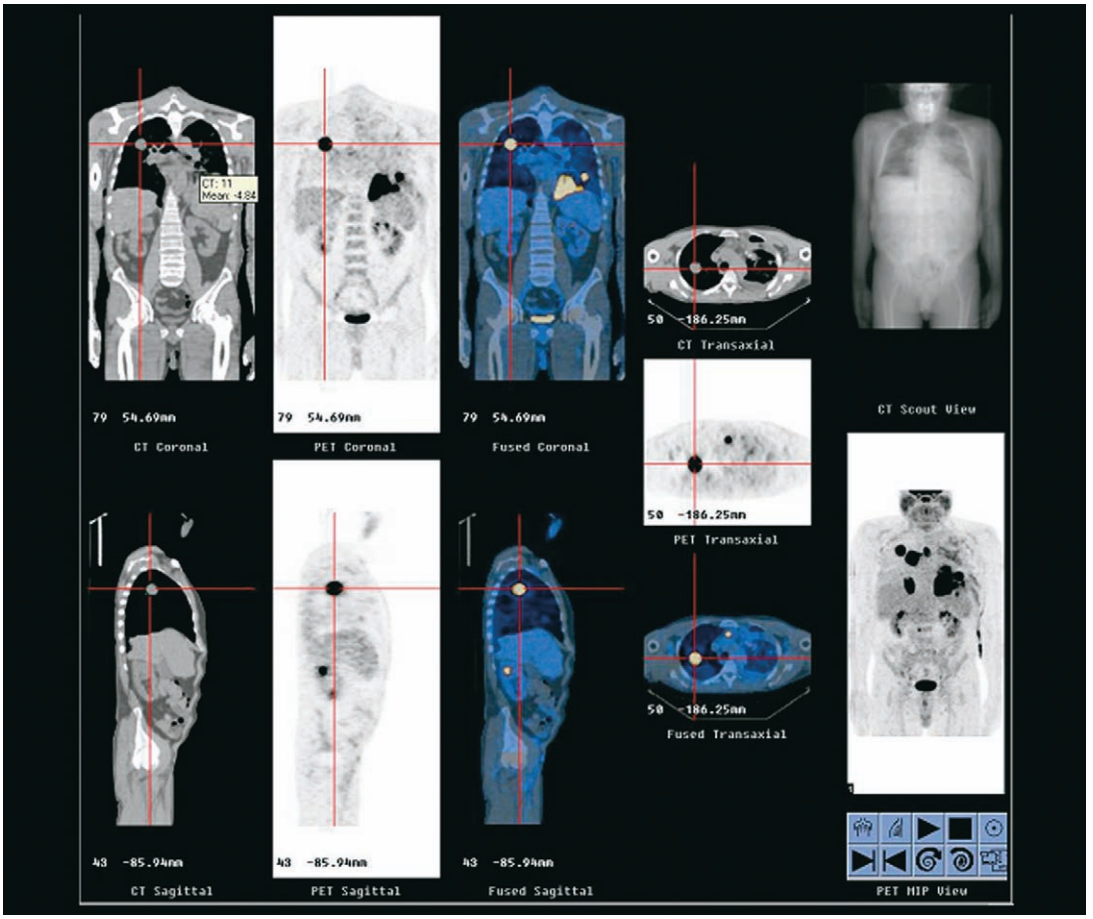

Fig. 8. ^{18}FDG-PET, CT, and fusion images from a 50-year-old HIV+ man demonstrating a hypermetabolic mass in the right lung and mediastinal lymphadenopathy and infradiaphragmatic disease. Diagnosis: non-Hodgkin's lymphoma. (Courtesy of Division of Nuclear Medicine, Department of Radiology, New York Presbyterian Hospital, Weill Cornell Medical Center, New York, NY).

umes were made in 25% of patients as a direct result of ^{18}FDG-PET imaging [65]. In addition, ^{18}FDG-PET differentiates scarring from residual or recurrent disease accurately. In one study it was more sensitive than, and as specific as, other modalities employed for this purpose. In a study of 63 patients suspected of NSCLC relapse, results of ^{18}FDG-PET and conventional evaluation methods were discordant in 43 patients. In 39 patients (91%), ^{18}FDG-PET was correct, resulting in major changes in the diagnosis in 25 patients (59%) [66]. To maximize the accuracy of the study, ^{18}FDG-PET should be performed 2 months after surgery and 4 to 6 months after radiotherapy [67].

Although prognosis in NSCLC is determined primarily by disease stage, tumor aggressiveness and invasiveness—and even metabolic activity—might also be important factors. Some data indicate that patients who have more intense uptake of ^{18}FDG have a shorter survival time. Other data have shown that patients who have persistent or recurrent abnormalities have shorter survival times than patients who have negative follow-up studies [66,68].

Fluorodeoxyglucose–positron emission tomography and other thoracic tumors

Increased anaerobic glucose metabolism, which is the basis for ^{18}FDG identification of carcinoma of the lung, is a feature of other malignant tumors of the thorax (Figs. 6–8). Accordingly, identification

of an ^{18}FDG-avid mass does not exclude metastatic foci from other adenocarcinomas, lymphoma, thyroid carcinomas, or even active necrotizing granulomas. The nuclear medicine physician should be provided with pertinent patient clinical history to be able to fully assess the likely etiology of the findings on the PET images. Likewise, the nuclear medicine physician should evaluate the ^{18}FDG images from the neck to the mid-thigh to fully assess the extent of disease and to identify other clinical conditions that might be present.

Summary

Over the past decade a variety nuclear medicine imaging studies have become available that are of considerable value to patients who have pulmonary malignancies. By far the greatest impact on the management of patients who have thoracic malignancy has been the availability of ^{18}FDG-PET imaging. In the patient who has newly diagnosed lung carcinoma, ^{18}FDG-PET improves the accuracy of staging the disease by identifying or excluding mediastinal disease and distant metastatic foci. ^{18}FDG-PET is superior to anatomic methods for evaluating the response to therapy and for distinguishing recurrent disease from posttreatment changes. Studies are in progress to evaluate the role of ^{18}FDG-PET imaging in assessing prognosis.

In patients who have bronchial carcinoid, somatostatin receptor imaging with ^{111}In-DTPA-pentetreotide (Octreoscan) can help identify patients who are candidates for curative surgery, detect unsuspected metastatic spread, and identify patients who might benefit from certain types of medical therapy. Although it was initially speculated that ^{18}FDG-PET imaging would not be sensitive for tumor detection in patients who have neuroendocrine tumors because of the usual slow metabolism and biology of these tumors, many neuroendocrine tumors are positive on ^{18}FDG-PET imaging. Nevertheless, there has been no direct comparison of ^{18}FDG-PET imaging and somatostatin receptor imaging, nor does a positive or negative ^{18}FDG-PET image exclude neuroendocrine tumor.

^{18}FDG-PET imaging and somatostatin receptor imaging with ^{99m}Tc-depreotide (Neotect) are safe, cost-effective methods that are valuable in the diagnosis and management of patients who have suspected or known lung cancer. ^{18}FDG-PET and ^{99m}Tc-depreotide imaging have a high degree of sensitivity, specificity, overall accuracy, and positive and negative predictive values in the evaluation of the solitary pulmonary nodule. These agents provide noninvasive, cost-effective methods for selecting patients for aggressive intervention without contributing to increased morbidity. Both methods have incremental value over CT imaging in selecting patients who have solitary pulmonary nodules for invasive biopsy or for thoracotomy.

References

[1] Coleman RE, Laymon CM, Turkington TG. FDG imaging of lung nodules: a phantom study comparing SPECT, camera-based PET, and dedicated PET. Radiology 1999;210:823–8.

[2] Gould MK, Maclean CC, Kuschner WG, et al. Accuracy of positron emission tomography for diagnosis of pulmonary nodules and mass lesions: a meta-analysis. JAMA 2001;285:914–24.

[3] Lardinois D, Weder W, Hany TF, et al. Staging of non-small-cell lung cancer with integrated positron-emission tomography and computed tomography. NEJM 2003;348:2500–7.

[4] Goldsmith SJ, Bar-Shalom R, Kostakoglu L, Weiner R, Neumann R. Gallium-67 scintigraphy in tumor detection. In: Sandler M, Coleman R, et al, editors. Diagnostic nuclear medicine. Philadelphia: Lippincott Williams & Wilkins; 2002. p. 911–9.

[5] Waxman AD. Thallium-201 and technetium-99m methixyisobutyl isonitrile (MIBI) in nuclear oncology. In: Sandler M, Coleman R, et al, editors. Diagnostic nuclear medicine. Philadelphia: Lippincott Williams & Wilkins; 2002. p. 931–47.

[6] Kostakoglu L, Goldsmith SJ. Imaging multidrug resistance in hematological malignancies. Hematology 2001; 6:111–24.

[7] Behr TM, Gotthardt M, Barth A, Behe M. Imaging tumors with peptide-based radioligands. Q J Nucl Med 2001;45:189–200.

[8] Reubi JC. Regulatory peptide receptors as molecular targets for cancer diagnosis and therapy. Q J Nucl Med 1997;41:63–70.

[9] Krenning EP, Kwekkeboom DJ, Pauwels S, Kvols LK, Reubi JC. Somatostain receptor scintigraphy. In: Freeman LM, editor. Nuclear medicine annual 1995. New York: Raven Press; 1995. p. 1–50.

[10] Krenning EP, Kwekkeboom DJ, Bakker WH. Somatostatin receptor scintigraphy with [^{111}In-DTPA-*D*-Phe1]- and [^{123}I-Tyr3]-octreotide: the Rotterdam experience with more than 1000 patients. Eur J Nucl Med 1993; 20:716–31.

[11] Bohuslavizki KH, Brenner W, Gunther M, et al. Somatostatin receotor scintigraphy in the staging of small cell lung cancer. Nucl Med Coomun 1996;17: 191–6.

[12] Fanti S, Farsard M, Battista G, et al. Somatostatin receptor scintigraphy for bronchial carcinoid follow-up. Clin Nucl Med 2003;28:548–52.

[13] O'Byrne KJ, O'Hare NJ, Freyne PJ, et al. Imaging of bronchial carcinoid tumors with indium-111 pentetreotide. Thorax 1994;49:284–6.
[14] Musi M, Carbone RG, Bertocchi C, et al. Bronchial carcinoid tumors: astudy on clinicopathological features and role of octreotide scintigraphy. Lung Cancer 1998;22:97–102.
[15] Blum JE, Handmaker H, Rinne NA. The utility of a somatostatin-type receptor binding peptide in the evaluation of solitary pulmonary nodules. Chest 1999;115: 224–32.
[16] Blum JE, Handmaker H, Lister-James J, et al. A multicenter trial with a somatostatin analog ^{99m}Tc-depreotide in the evaluation of solitary pulmonary nodules. Chest 2000;117:1232–8.
[17] Gambhir SS, Shephard JE, Handmaker H, Blum J. Analysis of the cost effectiveness of a somatostatin analog-Tc99m-Depreotide (Neotect) in the scintigraphic evaluation of solitary pulmonary nodules (SPN). J Nucl Med 1999;40(Suppl):57P.
[18] Boring CC, Squires TS, Tong T. Cancer statistics, 1992. CA Cancer J Clin 1992;42:19–38.
[19] Parker SL, Tong T, Bolden S, Wingo PA. Cancer statistics, 1997. CA Cancer J Clin 1997;47:5–27.
[20] Ost D, Fein A. Evaluation and management of the solitary pulmonary nodule. Am J Respir Crit Care Med 2000;162:782–7.
[21] Ward HB, Pliego M, Diefenthal HC, Humphrey EW. The impact of phantom CT scanning on surgery for the solitary pulmonary nodule. Surgery 1989;106:734–8.
[22] Salathe M, Soler M, Bolliger CT, et al. Transbronchial needle aspiration in routine fiberoptic bronchoscopy. Respiration (Herrlisheim) 1992;59:5–8.
[23] Schenk DA, Bower JH, Bryan CL, et al. Transbronchial needle aspiration staging of bronchogenic carcinoma. Am Rev Respir Dis 1986;134:146–8.
[24] Santambrogio L, Nosotti M, Bellaviti N, Pavoni G, Radice F, Caputo V. CT-guided fine- needle aspiration cytology of solitary pulmonary nodules: a prospective, randomized study of immediate cytologic evaluation. Chest 1997;112:423–5.
[25] Patz EJ, Lowe VJ, Hoffman JM, et al. Focal pulmonary abnormalities: evaluation with F-18 fluorodeoxyglucose PET scanning. Radiology 1993;188:487–90.
[26] Lowe VJ, Fletcher JW, Gobar L, et al. Prospective Investigation of positron emission tomography in lung nodules. J Clin Oncol 1998;16:1075–84.
[27] Kubota K, Matsuzawa T, Fijiwara T, et al. Differential diagnosis of lung tumor with positron emission tomography: a prospective study. J Nucl Med 1990;31: 1927–32.
[28] Gupta NC, Maloof J, Gunel E. Probability of malignancy in solitary pulmonary nodules using fluorine-18-FDG and PET. J Nucl Med 1996;37:943–8.
[29] Patz Jr EF, Lowe VJ, Hoffman JM, et al. Persistent or recurrent bronchogenic carcinoma: detection with PET and 2-[F-18]-deoxy-D-glucose. Radiology 1994; 191:379–82.
[30] Duhaylongsod FG, Lowe VJ, Patz Jr EF, et al. Detection of primary and recurrent lung cancer by means of F-18 fluorodeoxyglucose positron emission tomography (FDG PET). J Thorac Cardiovasc Surg 1995; 110:130–9.
[31] Bury T, Dowlati A, Paulus P, et al. Evaluation of the solitary pulmonary nodule by positron emission tomography imaging. Eur Respir J 1996;9:410–4.
[32] Sazon DA, Santiago SM, Soo Hoo GW, et al. Fluorodeoxyglucose-positron emission tomography in the detection and staging of lung cancer. Am J Respir Crit Care Med 1996;153:417–21.
[33] Prauer HW, Weber WA, Romer W, et al. Controlled prospective study of positron emission tomography using the glucose analogue [18f] fluorodeoxyglucose in the evaluation of pulmonary nodules. Br J Surg 1998;85:1506–11.
[34] Bury T, Rigo P. Contribution of positron emission tomography for the management of lung cancer. Rev Pneumol Clin 2000;56:1506–11.
[35] Higashi K, Ueda Y, Seki H, et al. Fluorine-18-FDG PET imaging is negative in bronchiolo-alveolar lung carcinoma. J Nucl Med 1998;39:1016–20.
[36] Farquar TH, Llacer J, Sayre J, et al. ROC and LROC analyses of the effects of lesion contrast, size, and signal-to-noise ratio on detectability in PET images. J Nucl Med 2000;41:745–54.
[37] Hoffman EJ, Huang SC, Phelps ME. Quantitation in positron emission computed tomography: 1. Effect of object size. J Comput Assist Tomogr 1979;3: 299–308.
[38] Wahl RL. Targeting glucose transporters for tumor imaging: "sweet" idea, "sour" result [editorial]. J Nucl Med 1996;37:1038–41.
[39] Roberts PF, Follette DM, von Haag D, et al. Factors associated with false positive staging of lung cancer by positron emission tomography. Ann Thorac Surg 2000; 70:1154–9.
[40] Kapucu LO, Meltzer CC, Townsend DW, et al. Fluorine-18-fluorodeoxyglucose uptake in pneumonia. J Nucl Med 1998;39:1267–9.
[41] Brudin LH, Valind SO, Rhodes CG, et al. Fluorine-18-deoxyglucose uptake in sacroidosis measured with positron emission tomography. Eur J Nucl Med 1994; 21:297–305.
[42] Bakheet SM, Saleem M, Powe J, et al. F-18 fluorodeoxyglucose chest uptake in lung inflammation and infection. Clin Nucl Med 2000;25:273–8.
[43] Matthies A, Hickeson M, Cuchiara A, Alavi A. Dual time point ^{18}F-FDG PET for the evaluation of pulmonary nodules. J Nucl Med 2002;43:871–5.
[44] Gambhir SS, Sheperd JE, Shah BD, et al. Analytical decision model for the cost-effective management of solitary pulmonary nodules. J Clin Oncol 1998;16: 2113–25.
[45] Dwamena BA, Sonnad SS, Angobaldo JO, et al. Metastases from non-small cell lung carcinoma: mediastinal staging in the 1990s—meta-analytic comparison of PET and CT. Radiology 1999;213:530–6.
[46] Webb WR, Gatsonis C, Zerhouni EA, et al. CT and

MR imaging in staging non-small cell bronchogenic carcinoma: report of the Radiologic Diagnostic Oncology Group. Radiology 1991;178:705–13.

[47] Steinert HC, Hauser M, Allemann F, et al. Non-small cell lung cancer: nodal staging with FDG PET versus CT with correlative lymph node mapping and sampling. Radiology 1997;202:441–6.

[48] Vansteenkiste JF, Stoobants SG, De Leyn PR, et al. Mediastinal lymph node staging with FDG PET scan in patients with potentially operable non-small cell lung cancer: a prospective analysis of 50 cases. Leuven Lung Cancer Group. Chest 1997;112:1480–6.

[49] Saunders CA, Dussek JE, O'Doherty MJ, et al. Evaluation of fluorine-18 fluorodeoxyglucose whole body positron emission tomography imaging in the staging of lung cancer. Ann Thorac Surg 1999;67:790–7.

[50] Kerstine KH, Stanford W, Mullan BF, et al. PET, CT, and MRI with Combidex for mediastinal staging in non-small cell lung cancinoma. Ann Thorac Surg 1999;68:1022–8.

[51] Weng E, Tran L, Rege S, et al. Accuracy and clinical impact of mediastinal lymph node staging with FDG PET imaging in potentially resectable lung cancer. Am J Clin Oncol 2000;23:47–52.

[52] Pieterman RM, van Putten JW, Meuzelaar JJ, et al. Preoperative staging of non-small cell lung cancer with positron-emission tomography. N Engl J Med 2000; 343:254–6.

[53] Bury T, Paulus P, Dowlati A, et al. Staging of the mediastinum: value of positron emission tomography imaging in non-small cell lung cancer. Eur Respir J 1996;9:2560–4.

[54] Martini N, Bains MS, Burt ME, et al. Incidence of local recurrence and second primary tumors in resected stage 1 lung cancer. J Thorac Cardiovasc Surg 1995;109: 120–9.

[55] Weder W, Schmid RA, Bruchhaus H, et al. detection of extrathoracic metastases by positron emission tomography in lung cancer. Ann Thorac Surg 1998;66:886–92.

[56] Bury T, Dowlati A, Paulus P, et al. Staging of non-small cell lung cancer by whole- body fluorine-18 deoxyglucose positron emission tomography. Eur J Nucl Med 1996;23:204–6.

[57] Erasmus JJ, Patz Jr EF, McAdams HP, et al. Evaluation of adrenal masses in patients with bronchogenic carcinoma using ^{18}F-fluorodeoxyglucose positron emission tomography. Am J Roentgenol 1997;168:1357–60.

[58] Bury T, Barreto A, Daenen F, et al. Fluorine-18 deoxyglucose positron emission tomography for the detection of bone metastases in patients with non-small cell lung cancer. Eur J Nucl Med 1998;25:1244–7.

[59] Schmirreister H, Guhlmann A, Eisner K, et al. Sensitivity in detecting osseous lesions depends on anatomic localization: planar bone scintigraphy versus ^{18}F PET. J Nucl Med 1999;40:1623–9.

[60] Meyer M, Gast T, Raja S, Hubner K. Increased F-18-FDG accumulation in an acute fracture. Clin Nucl Med 1994;19(1):13–4.

[61] Hustinx R, Paulus P, Jacquet N, et al. Clinical evaluation of whole-body ^{18}F-fluorodeoxyglucose positron emission tomography in the detection of liver metastases. Ann Oncol 1998;9:397–401.

[62] Valk PE, Pounds TR, Hopkins DM, et al. Staging non-small cell lung cancer by whole-body positron tomographic imaging. Ann Thorac Surg 1995;60:1573–81.

[63] Marom EM, McAdams HP, Erasmus JJ, et al. Staging non-small cell lung cancer with whole-body PET. Radiology 1999;212:803–9.

[64] Lewis P, Griffin S, Marsden P, et al. Whole-body ^{18}F-fluorodeoxyglucose positron emission tomo-graphy in preoperative evaluation of lung cancer. Lancet 1994; 334:1265–6.

[65] Hicks RJ, Kalff V, MacManus MP, et al. ^{18}F-FDG PET provides high-impact and powerful prognostic stratification in staging newly diagnosed non-small cell lung cancer. J Nucl Med 2001;42:1596–604.

[66] Hicks RJ, Kalff V, MacManus MP, et al. The utility of ^{18}F-FDG PET for suspected recurrent non-small cell lung cancer after potentially curative therapy: impact on management and prognostic stratification. J Nucl Med 2001;42:1605–13.

[67] Erasmus JJ, Patz Jr EF. Positron emission tomography imaging in the thorax. Clin Chest Med 1999;20: 715–24.

[68] Patz Jr EF, Connolly J, Herndon J. Prognostic value of thoracic FDG PET imaging after treatment for non-small cell lung cancer. Am J Roentgenol 2000;174: 769–74.